RESEARCH INTERESTS

MEMBRANES, MACROMOLECULES AND THEIR INTERACTIONS

VIRUSES: ASSEMBLY, STRUCTURE AND ENERGETICS

SELF-ASSEMBLING COMPLEX FLUIDS

SURVEY

Our research in recent years has mostly been concerened with systems and phenomena of *biophysical* interest. Much of the research has focused on studying the *interactions between biomembranes and biopolymers* such as DNA and proteins. Among the topics investigated are the formation of cationic lipid-DNA complexes (lipoplexes), membrane-mediated interactions between integral proteins, membrane perforation by amphipathic peptides, and macroion-induced phase separation of mixed fluid membranes. Another major topic of current interest involves the energetic, structural and thermodynamic characteristics of *viruses*, e.g., DNA packaging in (and release from) bacterial viruses, and the complex assembly of animal viruses.

These research topics have naturally evolved from our more general and continuing interest in the statistical-thermodynamics of *self-assembling* systems and *complex fluids*. Following some basic comments on amphiphile self-assembly (see also: http://star.tau.ac.il/ãndelman/moked_ english.html) the survey below outlines the background and some of the research topics studied in the last several years, focusing mainly on DNA-lipid complexes and membrane-protein interactions. The work pertaining to viruses and the formation of membrane pores by amphipathic peptides are very briefly mentioned. Additional details can be found in the relevant publications.

SELF-ASSEMBLING COMPLEX FLUIDS

Complex fluids are complex because of the intricate coupling between the internal degrees of freedom of their constituent particles (e.g., micellar aggregates or polymers) and their macroscopic phase behavior, [1,2]. Aqueous micellar solutions of self-assembling amphiphilic molecules provide numerous examples of this coupling. At low concentrations, some amphiphiles spontaneously aggregate into small spherical micelles, others form elongated cylindrical (rodlike) micelles, whereas most phospholipids self-assemble ino extended (practically infinite) two-dimensional bilayers, [3–5]. Other lipid species prefer assembling into (“inverted”) hexagonal or cubic phases, [6].

The self-assembled aggregates appearing in dilute solution reflect the intrinsic preference of the constituent molecules for the particular packing geometry. As far as their growth properties are concerned, spherical micelles, cylindrical micelles and planar bilayers are zero-, one- and two-dimensional objects, respectively, [1]. Thus, in statistical-thermodynamic terms, the formation of bilayers is an ordinary 2D phase transition (lipid condensation), whereas the average size of 1D cylindrical micelles increases monotonically (as opposed to abruptly) with concentration, since there is no condensation transition in 1D systems, [7]. These notions are confirmed by numerous experiments.

Held together by relatively weak ("hydrophobic") forces, self-assembled aggregates may change their size, shape and state of aggregation upon increasing the total concentration of their constituent molecules, ρ. For instance, the average length of rodlike micelles in dilute solution increases as $\sqrt{\rho}$, [3,5,1]. Inter-micellar (primarily excluded volume) forces between the rods become important when their average length becomes comparable to their spatial separation. Initially, these interactions modify the micellar size distribution, but as the concentration keeps increasing a variety of phase transitions come into play. Unlike in ordinary fluids these phase transitions reflect a highly non-trivial coupling between the "chemical" (self-assembly) degree of freedom, inter-aggregate interactions and orientational and translational order, [1,8]. Some of the emerging phases, such as those involving "wormlike" (i.e., long and flexible) micelles and cross-linked micellar networks, exhibit unique thermodynamic, visco-elastic and dynamic behaviors.

Our original interest in self-assembling complex fluids has largely been inspired by the intricate coupling between the internal (molecular) and external (thermodynamic) degrees of freedom of the intercating self-assembled aggregates. In parallel to studying inter-micellar forces and phase transitions of self-assembled aggregates, molecular-level theories have been developed for analyzing the microscopic characteristics of the aggregates. In particular, a general statistical-thermodynamic theory has been formulated, allowing the calculation of (amphiphile) chain packing statistics in arbitrary confined enviroments, [7,1]. This theory has been used to evaluate a vareity of single molecule characteristics, (e.g., orientational bond order parameters and spatial distributions of chain segments), showing excellent agreement with experiment and large scale computer simulations.

A most significant application of the theory has been the derivation of explicit, molecular-level, expressions [7,9–11], for the elastic moduli appearing in Helfrich's continuum theory for the curvature elasticity of lipid membranes, [12]. Understanding the molecular origin of membrane elasticity, e.g., the chain length or lipid composition dependence of the bending rigidity and spontaneous curvature [7,11] is, of course, crucial for understanding biological membranes, [13].

Formulating a molecular-level theory for the interaction between lipid membranes and integral proteins, [14,7,15–17], has been a natural extension of the chain packing theory. Thus, in the mid-1990's, in parallel to the ongoing investigation of "non-biophysical" problems (e.g., cross linking of cylindrical micelles and their bending rigidity) much of our research effort has been directed towards "biophysically inspired topics".

Meanwhile, our work on membrane-protein interaction has been extended to account for lipid-mediated interactions between integral proteins of arbitrary size and shape, as well as the protein-mediated transition between different lipid phases, [16,17].

Much of our research in the last five years has focused on the study of *lipoplexes*, [18–22]. These are complexes of DNA and lipid membranes composed of cationic (CL) and nonionic ("helper") lipids. Many research groups are involved in intensive experimental research of lipoplexes owing to their potential use as gene delivery vectors. Their structural characteristics and thermodynamic phase behavior present many challenging theoretical questions, involving the formulation and solution of rather intricate electrostatic and statistical-thermodynamic models, [23–26]. Similarly complex electrostatic and thermodynamic questions arise regarding

the interaction between charged (peripheral) proteins and partially (oppositely) charged mixed membranes, [27–30]. Studying these, biologically important, systems constitutes a major direction of our current research, as outlined in the next few sections.

Amphipathic, anti-microbial, peptides, are of considerable medical interest as antibiotic drugs, [31–35] Their interactions with lipid membranes combine many of the questions pertaining to lipid-protein interaction in general, but involve some rather subtle aspects of the competition between electrostatic and hydrophobic interactions. This, relatively new research topic in our group is only briefly mentioned toward the ned of this survey, (see, however, [36]). Another novel research project which is only briefly discussed below pertains to the packing characteristics of DNA (and RNA) in viral capsids and their transport across lipid membranes, [37,38]. Currently our virus research focuses on the assembly characteristics of animal viruses.

MEMBRANES, MACROMOLECULES AND THEIR INTERACTION

The lipid bilayer, constituting the central structural element of biological membranes, is a *flexible, self-assembled, two-dimensional fluid mixture*. These characteristics, generally synergistically, play crucial roles in the interaction between biomembranes and biopolymers such as proteins and DNA.

Being *flexible*, i.e., elastic with respect to bending deformations, the bilayer can respond to interactions with both peripheral and intrinsic macromolecules through local variations in its curvature. Changes in membrane area (and hence thickness) are also possible, but usually involve a higher energetic cost. Under certain conditions the local variations can develop into global (phase) ones, as discussed below. A local change in membrane structure occurs, for example, whenever a hydrophobic protein is inserted into a lipid bilayer. Invariably, this process involves a loss of conformational entropy of the felxible lipid chains surrounding the hydrophobic inclusion. The perturbation free energy is even larger in the case of "hydrophobic mismatch", i.e., when the protein length does not match the thickness of the unperturbed membrane, [14,16,39–41]. In this case, the lipid chains must stretch (or compress) in order to bridge over the (energetically highly unfavorable) hydrohpobic mismatch. In multicomponent lipid bilayers, as is usually the case in biological membranes, lipid chains of matching length can migrate toward the integral protein[42], thus lowering the elastic perturbation free energy, but at a certain cost of lipid mixing entropy.

The membrane perturbation free energy associated with an isolated hydrophobic protein is proportional to the number of chains in its immediate neighbourhood and hence to its circumference. This implies a *membrane-mediated* attraction between the proteins, because the total perturbation energy is lowered when two or more proteins stick to each other , [43]. If large enough, this attraction can compensate for the entropy loss associated with protein aggregation, resulting in a 2D condensation of proteins within the membrane plane.

More drastic changes in membrane structure and composition take place upon mixing DNA and liposomal bilayers containing cationic lipids (CL). (Liposomes, or vesicles, are closed, typically spherical, bilayer shells whose diameter can range from several tens of nanometrs to micrometers.) This mixing results in the spontaneous formation of the lipoplexes mentioned in the previous section, [18]. Fig. 1 depicts three types of complexes whose structure has been determined by a variety of experimental methods, including synchrotron X-ray diffraction [19, 20] and cryo-TEM [21,22].

Neglecting small edge effects, lipid bilayers, DNA and the lipoplexes can be regarded as macroscopic phases, (all embedded in the aqueous solution of course). Thus, thermodynamically, lipoplex formation is a first order phase transition. But the transition is of rather special kind, because the newly formed composite structure is not just a denser or differently ordered phase of the same particles (as is the case in ordinary changes of state). For instance, the hexagonal ("honeycomb") complex in Fig. 1B is formed by mixing planar lipid bilayers with

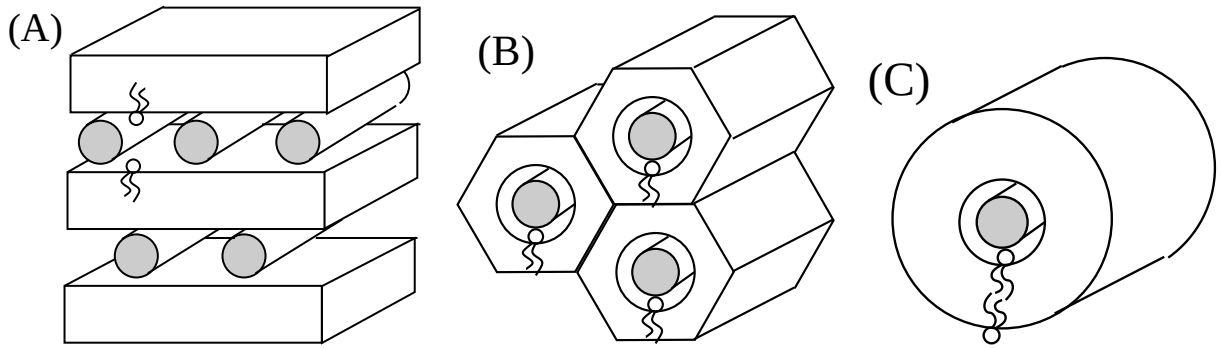

Figure 1. Structural models of three lipoplex geometries. A. A lamellar, "sandwich" (L^{c}_{α}), complex consisting of a smectic-like stack of charged bilayers with monolayers of parallel DNA rods (shaded cross sections) interacalated within the intervening water gaps. B. An hexagonal, "honeycomb" (H^{c}_{II}), complex consisting of an inverse-hexagonal lipid array, interacalating the DNA molecules within its cylindrical aqueous tubes. C. The "spaghetto" complex is a double stranded DNA molecule enveloped by a lipid bilayer.

DNA molecules. Actually, in some respects, lipoplex formation resembles a chemical reaction. When the total amount (more precisely charge) of DNA is larger than that of the total amount of (oppositely charged) lipid molecules, complexes of rather well defined stoichiometry coexist with uncomplexed DNA in solution, (resembling a chemical reaction $A + B \rightarrow AB$ when $[a] \gg [B]$). This optimal stoichiometry, indicating maximal stability of the complexes, is achieved at the *isoelectric* point. At this point the total number of negative (DNA) surface charges in the complex is exactly equal to the total number of positive (membrane) surface charges. (Complxes are also stable in a narrow region around the isoelectric point.)

What is so special about the isoelectric point?

Recall that prior to their association into a complex each of the two macroions (DNA and membrane) is surrounded by a cloud of oppositely charged, salt ions. These "weakly bound" counterions are spatially confined and their translational entropy content is negligible compared to free ions in solution. When two macroions (whose translational entropy is of course negligible) associate into a complex, not all counterions are needed any longer. In particular, at the isoelectric point essentially all counterions (of both macroions) can be releases into the bulk solution. This *counterion release* is the major driving force for macroion association in solution. In other words, the origin of the electrostatic attraction between the macroions is actually entropic. Consistent with this notion is the fact that macroion attraction decreases upon increasing the salt concentration in solution. This may be interpreted as due to charge screening or, equivalently, to the lower entropy gain of counterion release into a concentrated solution. Direct experimental evidence for counterion release in macroion association has recently been provided by conductivity measurements, revealing complete release at the isoelectric point, [26],(see also below).

All lipoplex geometries in Fig. 1 are stabilized by the electrostatic attraction between the negatively charged DNA molecules and the positively charged lipid bilayers. Their different geometries must reflect different elastic and packing characteristics of the lipid molecules. Indeed, bilayers of high bending rigidity will tend to keep their planar geometry and form lamellar ("sandwich") complexes, as depicted in Fig. 1A. On the other hand, "soft" ("easy to bend") bilayers will prefer the hexagonal ("honeycomb") geometry – mainly because it provides better electrostatic neutralization of DNA charges by the charged lipid headgroups, [25].

The "spaghetto" complex described in Fig. 1C consists of a single double stranded (ds) DNA, tightly enveloped by a cylindrical bilayer, [21,22]. Theoretical calculations reveal that

this complex is metastable with respect to the honeycomb complex shown in Fig. 1B, [23]. Noting that the two monolayers composing its bilayer mantle are oppositely curved, it follows that at least one of them is elastically "frustrated". It turns out that the unfavorably curved monolayer is the outer one. In the honeycomb complex which is composed of hexagonally packed "monolayer-coated DNA units", the system rids off the unfavorably bent outer layer of the spaghetti complexes. However, this process involves a substantial energetic barrier, explaining the kinetic stability of the spaghetti lipoplxes.

Since the membrane is a 2D *fluid mixture* the lipid molecules are free to diffuse within the bilayer plane. We have already mentioned that in a membrane containing a hydrophobic protein, lipids of matching length can diffuse towards the protein so as to avoid hydrophobic mismatch. Similar, local modulation of membrane composition take place when the membrane interacts with peripheral macromolecules. Consider for example the lamellar lipoplex in Fig. 1A, in which the negative charges are concentrated along the DNA rod. Attempting to neutralize these charges the cationic lipids migrate, within the membrane plane, towards (or away from) the DNA; minimizing the interaction free energy when the charge densities on the DNA and mambrane surfaces are equal, [44]. On the other hand, this, electrostatically driven segregation, is opposed by the loss of 2D mixing entropy. The actual composition (charge) profile is determined by a delicate interplay between the electrostatic and entropic contributions to the lipoplex free energy, [24]. In the next section we will describe a theoretical method which enables a self-consistent treatment of the electrostatic-entropic coupling, enabling a calculation of the membrane composition profile and, of course, the interaction free energies.

Using similar methods one can account for the role of surface charge (composition) modulations in the adsorption of (typically basic) proteins (or "protein domains") onto biological membranes containing a certain fraction of oppositely charge (usually acidic) lipids, [27,29]. As will be described in Sec. D, the adsorption characteristics on the "annealing" membrane surface are very different from those on "frozen" solid surfaces, [30,28]. In Sec. D we shall also comment on the conditions favoring global phase separation in the membrane, i.e., the appearance of a membrane domain rich in adsorbed proteins and charged lipid coexisting with a protein poor, weakly charged, membrane phase.

Above we have briefly described how the lipid membrane interacts with either hydrophobic-integral proteins or electrically charged i.e., peripheral proteins. Many proteins involve both hydrophobic and hydrophilic domains. A rather specific and important class of such proteins are the *amphipathic peptides* (e.g., megainin, melittin and alamethicin) which have been mentioned in Sec.A. Our work on this topic is outlined in Sec. F.

The cationic lipids in lipoplexes act as "condensing agents" for the highly charged DNA molecules. Nature uses other molecules for DNA compactization such as histon proteins in chromatin and polyvalent cations (e.g., the polyamines spermine and spermidine) in bacterial viruses (bacteriophages). Actually, the density of dsDNA within the protein shell (capsid) of most bacteriophages is enormous, giving rise to an extremely high internal pressure. We have recently analyzed the loading and ejection characteristics of bacteriophages, taking into account inter-strand interactions and DNA bending energies, finding excellent agreement with experiment, [**?**]. Our plan, as oulined in Sec. F is to extend our work to animal viruses. Unlike bacteriophages, the protein capsids of these viruses are enveloped by a lipid bilayer. Furthermore, whereas bacteriophages inject their genome through receptors on the bacteria membrane, animal viruses cross the cell via endo- and exo-cytosis events. This brings us again to our favorite research field of macromolecule-membrane interactions.

Lipid-DNA Complexes

Our first study of lipid-DNA complexes has been concerned with the 'spagghetto' and 'honeycomb' complexes shown in Fig. 1, [23]. At that time the existence of these complexes

has been conjectured on the basis of electron micrographs [21,22,45] but their actual geometry has not yet been determinded. X-ray diffraction studies on the honeycomb complex were published only a year later [20], revealing the structure in Fig. 1B. Our (independent) calculations predicted predicted very accurately the X-ray determination of the structure of hexagonal complexes. Furthermore, these experiments corroborated our predictions regarding the conditions (i.e., the nature of the lipid species) favoring one aggregation geoemtry over another, and the nature of the phase transitions betwen them. About a year later we have presented a detailed theoretical-computational study of the structure and thermodynamics of the lamellar complexes, again showing excellent agreement with the X-ray measurements, [24]. A comprehensive study of the (very complex) phase behavior of DNA/cationic lipid/nonionic lipid has been published in the year 2000, [25].

Our interest in the spaghetti and homeycomb complexes has been largely motivated by the fact that their formation, stability and phase behavior is governed by the intricate coupling between electrostatic, elastic (membrane curvature) and chemical (lipid composition) free energies. We have analyzed this coupling using (the nonlinear) Poisson-Boltzmann theory[46,5,47] for the electrostatic interactions, appropriately extended to account for local modulations of lipid composition, [24,30] (see below). Curvature elasticity was treated using the phenomenological theory (Helfrich's [12]) of membrane elasticity, and the 2D lipid mixing was treated in the level of "regular solution" theory. The details of these calculations are given in [25]. Qualitative insight into the factors governing the structure of the curved complexes can be gained in terms of a rather simple "capacitor" model [23], as outlined next.

The unit cell of the hexagonal complex (Fig. 1B) is a single dsDNA rod surrounded by a mixed cationic/nonionic lipid monolayer. (Wrapping this structural unit by another, oppositely curved monolayer, we obtain the spaghetto complex in Fig. 1C.) Accepting the notion that complex stability is maximal at isoelectricity it follows that the total charge on the DNA is exactly balanced by the cationic charge on the surface of the lipid monolayer surrounding it. In other words, the monolayer coated DNA unit is actually a concentric cylindrical *capacitor*. Its inner surface is that of the DNA , modeled as a rod of radius R^D and surface charge density σ^D. The outer cylinder, of *adjustable* radius R^I and surface charge density $\sigma^I = \sigma^D R^D/R^I$ is the lipid surface. Since the monolayer is elastic, R^I can asjust so as to minimize the sum of electrostatic and elastic contributions to the free energy of the unit cell. Both the capacitor charging energy and the elastic energy can be expressed in (simple) closed form, [23]. For lipid monolayers whose relaxed geometry is planar (zero spontaneous curvature, see below) one finds the optimal monolayer radius

$$R^I = \frac{\pi\kappa}{k_B T l_B} l^2 \tag{1}$$

with $l_B \approx 7$ Å denoting the Bjerrum length, and $l = 1.7$ Å is the average separation between phosphate charges, measured along the DNA axis. For a typical monolayer bending rigidity of $\kappa = 10\ k_B T$ (see e.g., [48]) we obtain $R^I = 12.7$ Å, just slightly larger than the DNA radius $R^D \approx 10$ Å. Lower κ implies smaller R^I, however lower monolayer radius is clearly impossible (because the difference $R^I - R^D \approx 3$Å is barely enough for one water layer). In fact, it turn out that for $\kappa \geq 10 k_B T$ the elastic deformation energy is large enough to favor the lamellar complex over the hexagonal one, despite the slightly lower electrostatically energy of the latter.

In mixtures of DNA with lipid bilayers of (relatively) large bending rigidities the phase behavior is quite simple because only lamellar complexes appear in solution. Fig. 2 illustrates, schematically, how the phases evolve as a function of ρ, the ratio between the total numbers of positive (lipid) and negative (DNA) surface charges of phases in solution. The curve marked d shows how the DNA-DNA distance within the complex varies with ρ. Such curves were determined by X-ray diffraction for a variety of lipid compositions and salt concentrations, [19, 49]. Our theoretical calculations of these curves revealed excellent agreement with the available

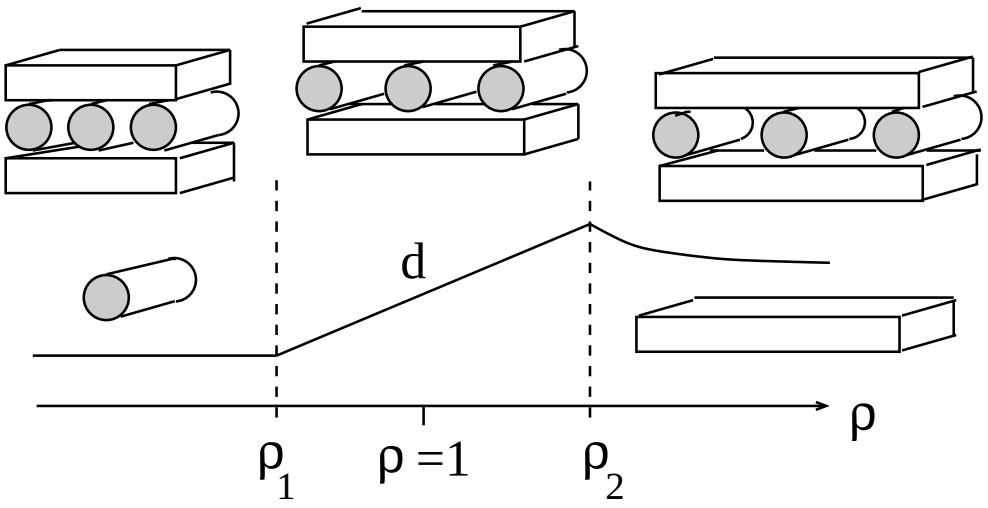

Figure 2. Schematic illustration of the phase behavior of lamellar CL-DNA self-assembled complexes. Shown is the DNA-to-DNA distance, *d*, as a function of lipid-to-DNA charge ratio, ρ. For $\rho < \rho_1$ uncomplexed DNA coexists with L_α^c complexes. For $\rho_1 \leq \rho \leq \rho_2$ the sytem proceeds through a one phase region where d is proportional to ρ. This narrow one-phase region (here largely maginifi ed) includes the isoelectric point $\rho = 1$ where the fi xed charges on the DNA and the cationic bilayer balance each other. For $\rho > \rho_2$ the L_α^c complexes coexist with excess cationic bilayers. The bilayer composition is generally different from that of the L_α^c complex.

experimental results, [24]. In fact, these calculations have also predicted several structural-thermodynamic properties (concerning e.g., the compositional modulation within the complex) which have later been confirmed experimentally, [50,51]. In the following we briefly outline the theoretical background underlying these calculations.

In order to evaluate the phase behavior of the system we first need the formation free energies of the complexes. A general free energy functional including all relevant contributions to the lipoplex free energy is given by:

$$\begin{aligned} F &= \int_v \frac{\epsilon}{2} \left(\nabla\Phi\right)^2 dv \\ &+ k_B T \int_v \left[n_+ \ln \frac{n_+}{n_0} + n_- \ln \frac{n_-}{n_0} - (n_+ + n_- + 2n_0) \right] dv \\ &+ \frac{k_B T}{a} \int_s \left[\eta \ln \eta + (1-\eta) \ln(1-\eta) \right] ds \\ &+ \chi \frac{k_B T}{a} \int_s \eta(1-\eta) ds \\ &+ \chi \frac{3 k_B T}{a} \int_s (\nabla\eta)^2 ds \\ &+ \int_s \frac{1}{2} \kappa(\eta) \left(c - c_0(\eta)\right)^2 ds \end{aligned} \tag{2}$$

The first term here is the electrostatic energy, with $\epsilon = \epsilon_0 \epsilon_r$ denoting the product of the permittivity of vacuum and the dielectric constant; $\Phi = e\Psi / k_B T$ is the reduced electrostatic potential, Ψ is the potential and e the elementary charge. The integration extends over the volume of the solution. The second term accounts for the entropy of mobile counterions in solution; n_+, n_- representing the local densities of the positive and negative (1:1) salt ions and n_0 their bulk

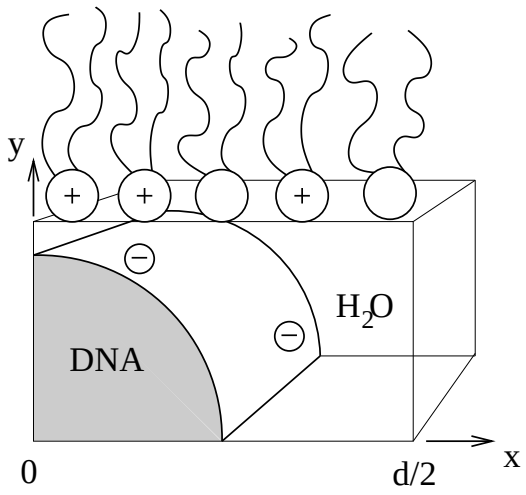

Figure 3. Schematic representation of one-quarter of the unit cell of a lamellar lipoplex. The (dimensionless) electrostatic potential $\Phi = \Phi(x, y)$ depends only on x and y, parallel and normal to the bilayer. The DNA surface is treated as being uniformly charged. On the other hand, the distribution of mobile cationic lipids can adjust along the x-axis so as minimize the free energy of the lipoplex. At this minimum the *electro-chemical* potential of the lipids is a constant independent of x, y

concentration.

Prior to describing the other terms in Eq. 2 it should be noted that minimization of F with respect to $n_\pm$ results in the familiar Poisson-Boltzmann (PB) equation,

$$\nabla^2\Phi = \kappa^2 \mathrm{sinh}\Phi \qquad ;\mathrm{where} \qquad \kappa = \frac{1}{l_D} = (\frac{2n_0e^2}{\epsilon_0\epsilon_r k_B T})^{1/2} \tag{3}$$

with l_D denoting the Debye screening length, (which, at high salt concentrations, denotes the distance beyond which Coulomb forces are screened by salt ions). Solving the PB equation subject to the appropriate boundary conditions yields Φ, using which we can calculate the free energy, the ion spatial distributions,$n_\pm(\mathbf{r})$, and other relevant quantities. In general the boundary conditions associated with surfaces of colloidal particles are either those of constant electrostatic potential or a constant (more precisely, given) surface charge density, [5,47]. This latter condition, in our problem is associated for example with the immobile DNA surface charges; see Fig. 3. On the other hand, the lipid charges at the membrane surface are *mobile*, and their "optimal" 2D distribution is dictated by the requirement that F is minimal.

The 2D mobility of the lipid molecules is accounted for by the third, fourth and fifth terms in Eq. 2, with $\eta = \eta(x, y)$ denoting the local density of the charged lipid, χ is the nonideality or interaction parameter (from the theory of concentrated solutions, see e.g., [52]), and a is the area per lipid at the membrane surface. All three integrals extend over the membrane area in the unit cell. For an ideal lipid mixture, which for many systems is a very good approximation, only the third term survives, representing the 2D lipid mixing entropy. The fourth and fifth contributions to F are relevant when the lipid mixture is nonideal, and the last one expresses the elastic energy associated with local changes in membrane curvature. We shall return to these terms in the next section.

For an *ideal* lipid mixture (as is often the case in lipoplexes) and a given complex geometry, the last three terms in F are irrelevant. Then, minimizing F with respect to $n_\pm$ *and* η, subject to the (lipid) charge conservation constraint,

$$\frac{1}{a}\int_S \eta ds = \langle\eta\rangle \tag{4}$$

we again obtain the PB equation, but we also get the boundary condition on the membrane suface

$$\eta = \frac{1}{1 + (\frac{1-\langle\eta\rangle}{\langle\eta\rangle})e^{(\Phi+\lambda)}} = -\frac{a\epsilon k_B T}{e^2}\hat{n}\nabla\Phi \tag{5}$$

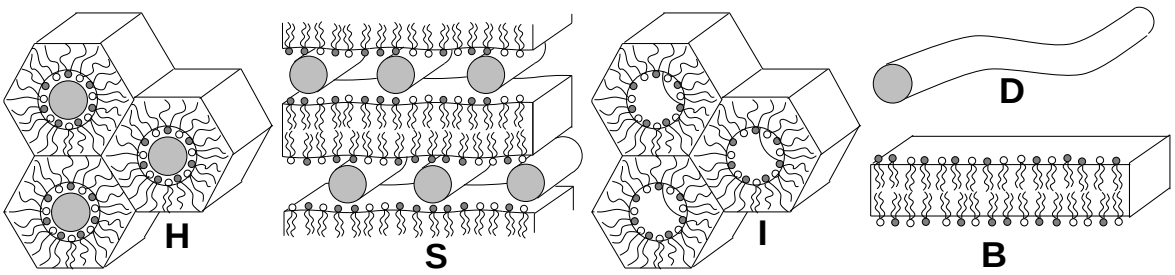

Figure 4. Schematic illustration of the five macroscopic phases relevant for evaluating the phase behavior of CL-DNA systems. The phases denoted by H and S are the hexagonal and lamellar lipolexes. The DNA-free structures I and B are the inverse-hexagonal and bilayer lipid phases, respectively. D represents uncomplexed DNA. The lipid layers are mixed, consisting of cationic and neutral (helper) lipids. See [25].

which expresses the condition for constant *electro-chemical potential* of the lipids anywhere in the system, [24]. The PB equation must be solved self-consistently with the boundary condition Eq. 5, yielding both Φ and the membrane charge density profile $\eta(\mathbf{r})$.

Our treatment above of the lipid mobility degree of freedom has been the first time that the fluid nature of the lipid membrane has been taken into account in a theoretical study of membrane-macromolecule interaction. How important is this degree of freedom? In a lamellar complex where the average fraction of charged lipid is $\langle\eta\rangle = 0.5$ the local charge density varies between $\eta = 0.65$ in the vicinity of the DNA and 0.35 at the midpoint between two neighboring strands, [24]. Furthermore, the complex stabilization energy is considerably higher than in a system where $\eta\langle\eta\rangle$ is forced to be constant; (a hypothetical scenario except for a membrane in the gel phase). These, charge polarization, effects increase as the average charge density of the membrane decreases. The origin of the effect is clear: the electrostatic interaction free energy between two oppositely charged surfaces is minimal when (the absolute values of) their charge desnities are equal, allowing complete release of the mobile counterions from the aqueous gap between the surfaces. In the lamellar complex, where the DNA charges are fixed, only the mobile lipid charges can lead to this condition. The actual charge profile $\eta(\mathbf{r})$ is a compromise between the electrostatic force for charge matching and the lipid mixing entropy which favors uniform mixing and hence opposes charge modulation, [24,30]. In the next section we shall see that similar, sometimes more dramatic effects, prevail in protein adsorption processes.

Once the formation free energies of all relevant structures are known, the theoretical determination of the thermodynamic phase behavior is, in principle, straightforward. One "only" has to write a free energy functional involving all possible structures in the system, e.g., those shown in Fig. 4. This functional is then minimized with respect to the relative proportions of the various phases, and subject to the material conservation ("lever") rules. Equivalently, one has to solve all the independent coexistence equations, expressing the equality of chemical potentials of every molecular species in all phase. For a multicomponent complex system such as ours this is a nontrivial, yet feasible task. We shall suffice here in mentioning that detailed phase diagrams have indeed been calculated this way, revealing generally rather complicated phase diagrams, involving a variety of phases and coexistence regimes, [25]. These phase diagrams can vary markedly from one type of lipid mixture to another, depending on the packing and elastic characteristics of the lipid constituents. These properties are generally known from independent measurements, allowing the prediction of reliable phase diagrams and thus providing useful information for the design of lipoplexes.

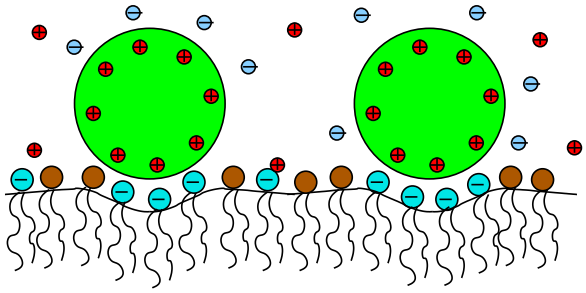

Figure 5. Lipid membranes are flexible 2D fluid mixtures. They can adapt to the shape and charge density of peripherally adsorbed proteins. Both the ensuing elastic membrane perturbations and lipid "polarization" effects increase the adsorption strength and give rise to membrane-mediated protein-protein interactions.

Electrostatic Adsorption of Proteins

Most cell membranes contain a small fraction of charged lipids, (typically around 10 percents of acidic lipids in their inner leaflet, [48]. Electrostatic adsorption of proteins (typically through basic domains) onto the lipid membrane plays an important role in a variety of biological (e.g., signal transduction) processes. Most, though not all (see e.g., [28]) of the (many) theoretical studies of protein adsorption published in the biophysical literature (see e.g., [27,29]) are based on the assumption that the lipid composition of the membrane is constant and spatially uniform, thus ignoring the ability of the charged lipids to migrate towards (or away from) an adsorbing protein/ This ability is illustrated schematically in Fig. 5, which also shows another possible response mechanism of the lipid membrane to macromolecule adsorption, namely, a local change in interfacial curvature [53,54]. These curvature modulations are accounted for by the last term in Eq. 2, where $\kappa(\eta)$ is the local (composition dependent) bending constant and $c_0(\eta)$ is the local spontaneous curvature, [11]. For a perfectly planar membrane, as will be assumed hereafter, this curvature term is irrelevant.

Figure 6 illustrates the adsorption of a basic globular protein, modeled as a uniformly charged sphere, onto the surface of a mixed bilayer containing anionic lipids, [30]. PB theory was used to calculate the adsorption free energy of the protein as function of the adsorption height h. The figure contrasts three calculations of the adsorption free energy and the charge modulation profile; all for an ideally mixed lipid mixture (whose F is given by the first three terms in Eq. 2) in the limit of low surface coverage. The smallest adsorption energy is for the hypothetical case of a "frozen" membrane composition. The largset adsorption energy and most dramatic charge modulation corresponds to a surface of constant electrical potential, as if the membrane was a metal conductor. A real fluid bilayer, however, corresponds to the "intermediate" case of *constant electro-chemical potential*, representing the compromise between the electrostatic tendency for charge polarization and the 2D lipid entropy (third term in Eq. 2) which opposed this demixing. The results of a representative calculation are shown in Fig. 6 (right), corresponding to 20% charged lipids in the membrane, a radius $R = 10$ Å of the protein sphere with 7 positive charges attached to its surface.

Comprehensive calculations based on Eq. 2 for the electrostatic adsorption energies and thermodynamic adsorption isotherms have been carried out for a wide range of conditions [30]. The adsorption isotherms explicitly account for electrostatic repulsions between the proteins, which become extremely strong once the distance between neighboring adsorbates falls below the Debye screening length.

It turns out that the lipid demixing effects in protein adsorption are particularly important for the biologically most relevant cases where highly charged proteins adsorb on weakly charged membranes.

Another issue of great importance in biological systems is the question whether protein adsoption can result in the formation of membrane "domains" characterized by a high concentration of adsorbed proteins and their "favorite" lipids, [27]. From a thermodynamic point of

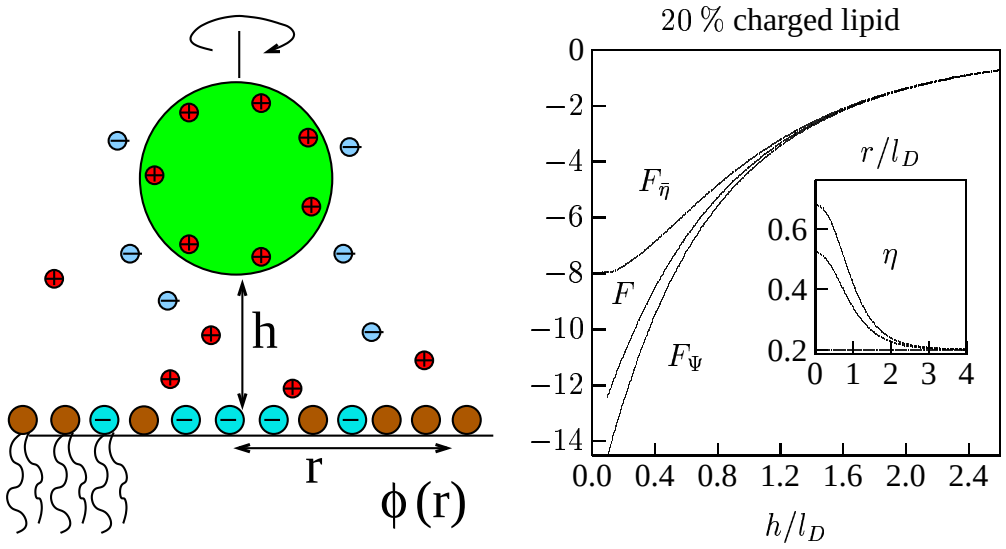

Figure 6. Left: a uniformly charged sphere adsorbs onto a flat, fluid, two-component membrane. The mobile lipids adjust their local composition (here denoted as $\phi(r)$, corresponding to $\eta(r)$ elsewhere) for any given protein-to-membrane distance h. Right: Predictions from PB theory for the adsorption of a single sphere (of radius $R = 10$ Å with a uniform charge density corresponding to 7 positive charges) onto a mixed membrane that contains 20% negatively charged lipids. The three adsorption free energies (in units of k_BT) correspond to fixed surface charge density ($F_{\bar{\eta}}$), constant electro-chemical potential (F), and constant membrane surface potential (F_Ψ). The inset shows the local membrane composition, η, for the three cases at $h/l_D = 0.3$. The Debye length is $l_D = 10$ Å.

view the formation of such domains (in certain contexts also referred to as “rafts”, [55,56]) is a two dimensional phase separation of the *protein-dressed membrane*. Much of our recent research efforts have focussed on the theoretical elucidation of this issue, as briefly outlined next.

Recall that an adsorbed macroion can induce a local adjustment of the lipid composition in its vicinity, thus forming an optimal protein-lipid “patch”. Such, “electrostatically-satisfied” patches can diffuse in the membrane plane, behaving as a 2D gas. The question then is why should these patches condense into a protein rich membrane domain, see Fig. 7. Clearly, for such a transition to take place the patches must attract each other. Since the adsorbed proteins are similarly charged, their direct interaction is repulsive, and we conclude that only the underlying lipid surface can mediate this attraction. We argue that a necessary requirement for this attraction is that χ, the nonideality parameter in Eq. 2, should be positive. In other words, the lipid chains of the charged and neutral lipids should tend to separate, thus favoring the local demixing occuring upon adsorption of individual macroions. In this case, the boundary between the lipid patch and its immediate surroundings involves an unfavorable “line energy”, Γ. This line energy can be shown to be proportional to the product of χ, the perimeter length of the protein-lipid patch, and the square of the gradient of the lipid composition profile, (as in the fifth term in Eq. 2). Domain formation takes place when Γ exceeds a a critical value, which may be either smaller or larger that the critical χ, depending on the protein size and charge and membrane charge density. A preliminary account of this work has recently appeared in print [57]..

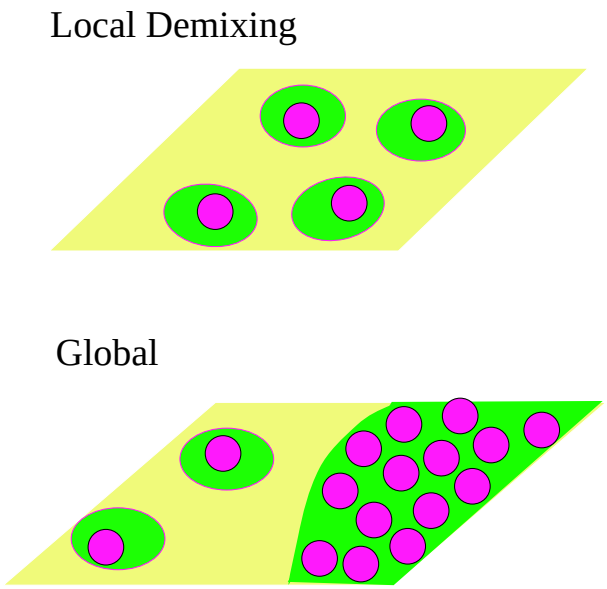

Figure 7. Top: Adsorbed proteins attract their favorite lipids, behaving like a 2D gas of protein-lipid "patches". Bottom: Under certain conditions (see text) the 2D gas condenses into protein-rich domains

Membranes and Integral Proteins

Notwithstanding the structural and functional variety of transmembrane proteins their skeleton is almost invariably much more rigid than the surrounding lipid membrane. The strong hydrophobic forces anchoring the protein into the membrane thus create an interface between a rigid membrane inclusion and the elastic and lipid enviroment. This interface involves an elastic perturbation free energy of the lipid chains, reflecting mainly a loss of conformational entropy by the lipid molecules bordering the inclusion. Additional contributions to the lipid perturbation energy arise in cases of nonzero *hydrophobic mismatch*; i.e., when the protein inclusion is longer or shorter than the thickness of the unperturbed lipid bilayer, [14,16,39–42]. The lipid perturbation energy is (roughly) proportional to the surface area of the inclusion. If large enough, it tends to favor protein aggregation, through membrane-mediated attraction, analogous to the attraction between peripheral proteins described at the end of the previous section.

In the past we have studied various aspects of the interaction between integral proteins and the host lipid membrane. We shall suffice here in brief mention of one recent study, in which a molecular-level elastic theory has been presented for the membrane-mediated interaction between hydrophobic inclusions of arbitrary size and shape, [16]. Among the major and novel applications of this approach has been the explanation of the peptide-mediated morphological transition of the lipid assembly from a lamellar (bilayer) phase to the inverse-hexagonal phase [39,58–60], as shown in Fig. 8. More explicitly, it was found that the channel protein gramicidin A and a number of short α-helical transmembrane peptides can induce a first order phase transition from a peptide-poor bilayer to a peptide-rich inverse-hexagonal phase. Using our molecular theory for lipid-protein interaction we have calculated the free energies of the two phases as a function of peptide/lipid concentration ratio. Then, equating lipid and peptide chemical potentials in the coexisting phases or, equivalently, using the common tangent construction (see Fig. 8), we have determined the phase boundaries. Indeed we found that once the amount of short peptides within a bilayer exceeds a certain (low) threshold concentration the system "jumps" into a peptide-rich hexagonal phase. The latter is stabilized by the presence

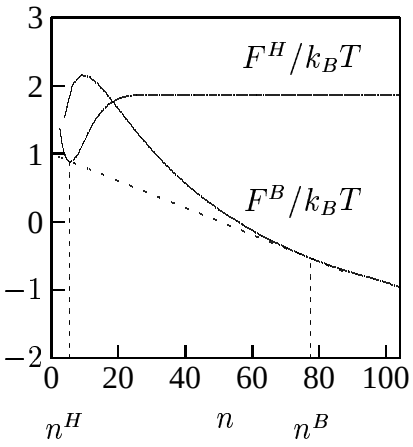

Figure 8. The free energy per peptide in the inverse hexagonal phase (F^H), and in the bilayer phase (F^B), as a function of the number of lipids per peptide, n. The compositions at coexistence, n^B and n^H, are detrmined by the common tangent construction. These calculations correspond to peptides whose hydrophic length is is two thirds of the unperturbed lipid bilayer, [16]

of the peptides in the ridges connecting neighboring unit cells. Our theory could adequately explain most of the relevant experimental results. (A special "new and notable" commentary by S. Marčelja has been published following our paper in the same issue of the Biophysical Journal, [61].)

Membranes and Amphipathic Peptides

Amphipathic α-helical peptides, often depicted as cylinders, involve a hydrophobic face (characterized by an angle θ, as viewed along the cylinder's axis) and a complementary polar, often charged, face (corresponding to the complementary angle, $2\pi - \theta$), [31–35]. Usually, they first adsorb onto the membrane with their polar face dipping into the hydrophobic core of the bilayer. Consequently, neighboring lipid chains must stretch and bend in order to fill up the space "underneath" the peptide, ensuring uniform density of chain segments within the hydrophobic core. The formation of an adsorbed peptide "carpet" results in membrane thinning, in a manner depending on peptide concentration and lipid chain characteristics. Above a certain critical concentration the peptides insert into the membrane to form trans-membrane pores, composed of several peptides, with their polar faces in contact with water. Some peptides, like (the weakly charged) alamethicin line up touching each other to form a *"barrel-stave"* pores. Others, like (the highly charged) magainin and melittin appear to form *"toroidal"* pores, where lipid headgroups intercalate between the peptides, providing partial screening of inter-peptide repulsion. and references therein).

Several theoretical models have been proposed to account for the interesting structural and statistical-thermodynamic behavior of these systems. Some of the structural models are based on continuum elastic theories, appropriate for long ranged perturbations, see e.g., [35,62]. Others employ atomic level simulations and are naturally restricted to a small number of specific systems, see e.g., [63]. Underlying our approach is an "intermediate", molecular-level, theory for both the adsorbed and pore states, allowing a general treatment of both electrostatic and chain-packing contributions.

We have recently completed a series of free energy calculations of pore states which (to the best of our knowledge for the first time) treat in a consistent and systematic fashion the electrostatic formation energies of peptide pores of varying sizes, [36]. The major qualitative result of these calculations is that all peptides except perhaps very weakly charged ones (e.g., alamethicin) should preferrably form toroidal rather than barrel-stave pores.

At present, detailed molecular-level ("chain packing") calculations are carried out to evaluate the elastic membrane deformation free energy associated with amphipathic peptide adsorption.

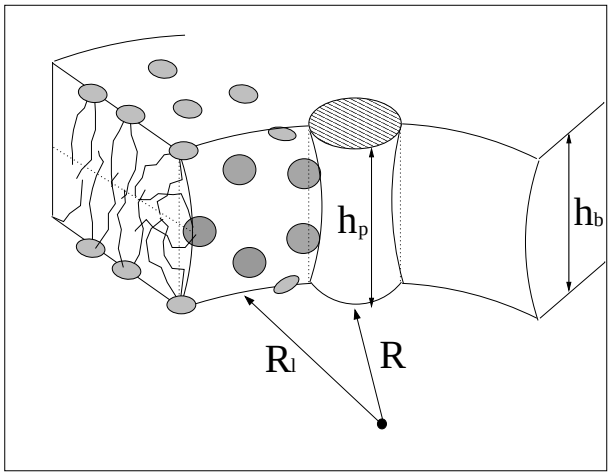

Figure 9. Schematic illustration of a section of a toroidal pore, see [36]

VIRUSES

A single double-stranded DNA (dsDNA) molecule in solution, in the presence of "condensing agents", collapses spontaneously into a tightly packed torus, see Fig. 10. Since DNA is highly negatively charged, the positively charged condensing agents, e.g., the short polyamines spermine or spermidine, serve as linkers between neighboring DNA strands within the torus. The size of the torus can be shown to depend on a subtle interplay between the cohesive energy due to the polyamine-mediated attraction between dsDNA which tends to condense it into a globule, (see e.g., [64]) and the rather high bending rigidity of DNA (persistence length of 50nm) which tends to keep it as a random coil. Typically, the large torus radius is on the order of 100nm, whereas the small radius is about 5nm. The optimal distance between the hexagonally packed dsDNA's is 2.8nm, [65].

The DNA within the (icosahedral) protein capsid of bacteriophages is packed at extremely high density. In fact, this density is so high that the interaxial distance between neighboring dsDNA's is approximately 2.5nm [66], i.e., on the repulsive part of the DNA-DNA interaction potential curve. Furthermore, unlike in solution where DNA is packed as a torus, such a torus is too large to fit into the confines of the capsid. Experiments suggest that it is packed there as a "spool", [65].

Following the initial ejection of DNA into solution, the portion still remaining in the capsid can relax and reorganize its structure, changing gradually from a spool to torus geometry; turning eventually into a small torus once its length falls below a certain critical value. Its portion outside the capsid, i.e., in solution, is that of a torus, whose size increases as the ejected length increases.

We have used two complementary approaches to investigate the evolution of structure and energetics along the loading coordinate [37,38]. Brownian Molecular Dynamics dynamics and an analytical theory based on a free energy expression including elastic, cohesive and surface terms. The forces, free energies and structures of the DNA inside and outside the capsid were calculated as a function of the ejected (equivalently, loaded) length. We found, using both approaches, that ejection takes place in two well defined stages, as illustrated schematically in Fig. 11. First the pressure inside the capsid is rapidly released, with a concomitant (continuous) transition from a spool to torus structure. Once the interaxial spacing becomes equal to that in solution, the ejection is much slower and governed by the surface energy terms (Ostwald

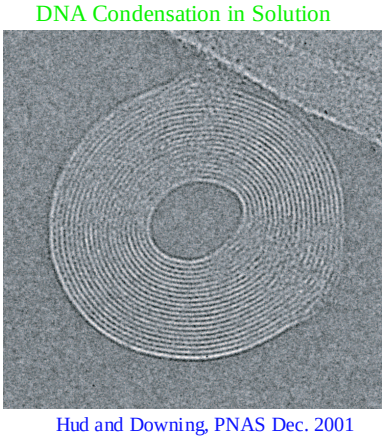

Figure 10. Electron micrograph of a (λ-DNA) torus in aqueous soltion containing polyamines, from [67]

ripening).

Our theorteical calculations of the DNA loading forces were carried out independently and in parallel to the first experimental determination of these forces by Bustamante and coworkers, [68]. The agreement between theory and experiment is very good.

Our current research directions focus on understanding the mechanisms of animal virus transport through cell membranes. These viruses, after replication, leave the cell via endocytosis in a process involving self-assembly on the inner cell membrane, budding deformation and membrane fission. These sequence of processes is mediated by a variety of cellular and membranal proteins and special lipid species. Preliminary theoretical models have already been formulated in order to study selected aspects of this complicated process. Two schematic illustrations, describing viral exocitosis are shown in Figures 12 and 13. The "CAN" (cytopsmically assembled) viruses complete their genome packaging while still in the cytoplasm, and become coated by a lipid membrane (with the help of spike proteins) on its way out of the cell. The other mechanism, corresponding to "MAN" (membrane assembled) viruses (such as the HIV and other retroviruses), involves the simulateneous organization of the genome (RNA), capsid proteins and the lipid membrane in the course of exocytosis.

REFERENCES

[1] Ben-Shaul, A. and Gelbart, W. M. In *Micelles, Membranes, Microemulsions and Monolayers*, Gelbart, W. M., Ben-Shaul, A., and Roux, D., editors, chapter 1, 359–402. Springer, New York (1994).

[2] Gelbart, W. M. and Ben-Shaul, A. *J. Phys. Chem.* **100**, 13169–13189 (1996).

[3] Israelachvili, J. N. *Intermolecular and Surface Forces*. Academic press, second edition, (1992).

[4] Israelachvili, J. N., Mitchell, J., and Ninham, B. W. *J. Chem. Soc. Farad. 2* **72**, 1525–1568 (1976).

[5] Evans, D. F. and Wennerström, H. *The Colloidal Domain, where Physics, Chemistry, and Biology Meet*. VCH publishers, second edition, (1994).

[6] Seddon, J. M. and Templer, R. H. In *Structure and Dynamics of Membranes*, Lipowsky, R. and Sackmann, E., editors, volume 1A, section 3, 98–160. Elsevier, Amsterdam (1995).

[7] Ben-Shaul, A. In *Structure and Dynamics of Membranes*, Lipowsky, R. and Sackmann,

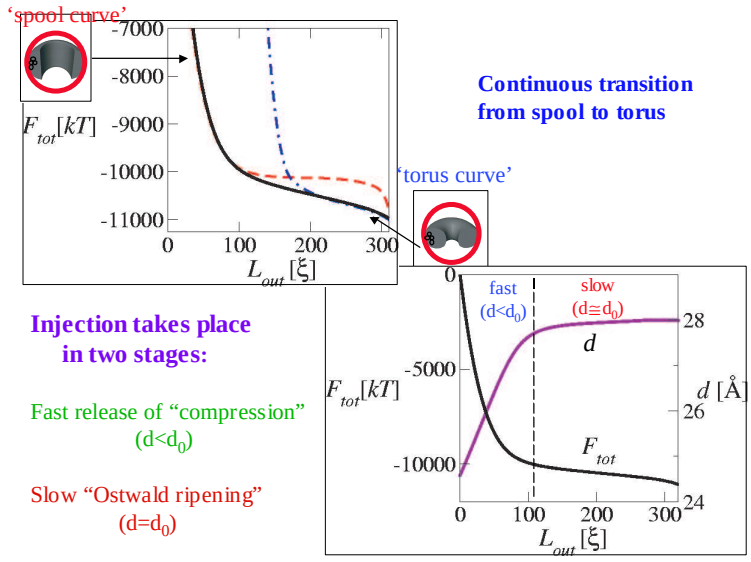

Figure 11. DNA injection from a bacteriophage takes place in two distinct stages, see [37,38]

E., editors, volume 1A, chapter 7, 359–402. Elsevier, Amsterdam (1995).

[8] Bohbot, Y., Ben-Shaul, A., Granek, R., and Gelbart, W. M. *J. Chem. Phys.* **103**, 8764–8782 (1995).

[9] Szleifer, I., Kramer, D., Ben-Shaul, A., Roux, D., and Gelbart, W. M. *Phys. Rev. Lett.* **60**, 1966–1969 (1988).

[10] Szleifer, I., Kramer, D., Ben-Shaul, A., Gelbart, W. M., and Safran, S. A. *J. Chem. Phys.* **92**, 6800–6817 (1990).

[11] May, S. and Ben-Shaul, A. *J. Chem. Phys.* **103**, 3839–3848 (1995).

[12] Helfrich, W. *Z. Naturforsch.* **28**, 693–703 (1973).

[13] Lipowsky, R. and Sackmann, E., editors. *Structure and Dynamics of Membranes*, Amsterdam, (1995). Elsevier.

[14] Fattal, D. R. and Ben-Shaul, A. *Biophys. J.* **65**, 1795–1809 (1993).

[15] Ben-Shaul, A., Ben-Tal, N., and Honig, B. *Biophys. J.* **71**, 130–138 (1996).

[16] May, S. and Ben-Shaul, A. *Biophys. J.* **76**, 751–767 (1999).

[17] May, S. and Ben-Shaul, A. *Phys. Chem. Chem. Phys.* **2**, 4494–4502 (2000).

[18] Felgner, P. L. *Scientific American* **276**, 102–106 (1997).

[19] Rädler, J. O., Koltover, I., Salditt, T., and Safinya, C. R. *Science* **275**, 810–814 (1997).

[20] Koltover, I., Salditt, T., Rädler, J. O., and Safinya, C. R. *Science* **281**, 78–81 (1998).

[21] Sternberg, B., Sorgi, F. L., and Huang, L. *FEBS Letters* **356**, 361–366 (1994).

[22] Sternberg, B. *J. Liposome Res.* **6**, 515–533 (1996).

[23] May, S. and Ben-Shaul, A. *Biophys. J.* **73**, 2427–2440 (1997).

[24] Harries, D., May, S., Gelbart, W. M., and Ben-Shaul, A. *Biophys. J.* **75**, 159–173 (1998).

[25] May, S., Harries, D., and Ben-Shaul, A. *Biophys. J.* **78**, 1681–1697 (2000).

[26] Wagner, K., Harries, D., May, S., Kahl, V., Rädler, J. O., and Ben-Shaul, A. *Langmuir* **16**, 303–306 (2000).

[27] Denisov, G., Wanaski, S., Luan, P., Glaser, M., and McLaughlin, S. *Biophys. J.* **74**, 731–744 (1998).

[28] Heimburg, T., Angerstein, B., and Marsh, D. *Biophys. J.* **76**, 2575–2586 (1999).

[29] Murray, D., Arbuzova, A., Hangyás-Mihályné, G., Gambhir, A., Ben-Tal, N., Honig, B., and McLaughlin, S. *Biophys. J.* **77**, 3176–3188 (1999).

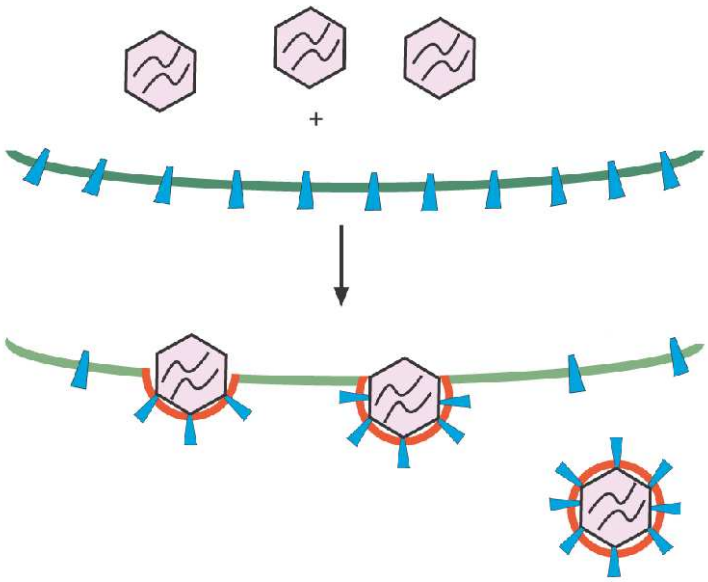

Figure 12. Schematic illustration of the budding mechanism of CAN (cytoplasm-assembled-nucleocapsids) viruses.

[30] May, S., Harries, D., and Ben-Shaul, A. *Biophys. J.* **79**, 1747–1760 (2000).

[31] Matsuzaki, K. *Biochim. Biophys. Acta.* **1462**, 1–10 (1999).

[32] Bechinger, B. *J. Memb. Biol.* **156**, 197–211 (1997).

[33] Shai, Y. *Biochim. Biophys. Acta.* **1462**, 55–70 (1999).

[34] Epand, R. M., Shai, Y., Segrest, J. P., and Anantharamaiah, G. M. *Biopolymers (Peptide Science)* **37**, 319–338 (1995).

[35] Harroun, T. A., Heller, W. T., Weiss, T. M., Yang, L., and Huang, H. W. *Biophys. J.* **76**, 3176–3185 (1999).

[36] Zemel, A., Fattal, D. R., and Ben-Shaul, A. *Biophys. J* (2003). in press.

[37] Kindt, J., Tzlil, S., Ben-Shaul, A., and Gelbart, W. M. *Proc. Nat'l. Acad. Sci. USA* **98**, 13671–13674 (2001).

[38] Tzlil, S., Kindt, J. T., Gelbart, W. M., and Ben-Shaul, A. *Biophys. J.* (2003). in press.

[39] Killian, J. A., Salemink, I., de Planque, M. R. R., Lindblom, G., Koeppe, R. E., and Greathouse, D. V. *Biochemistry* **35**, 1037–1045 (1996).

[40] Morein, S., Koeppe, R. E., Lindblom, G., de Kruijff, B., and Killian, J. A. *Biophys. J.* **78**, 2475–2485 (2000).

[41] Bloom, M., Evans, E., and Mouritsen, O. G. *Q. Rev. Biophys.* **24**, 293–397 (1991).

[42] Dumas, F., Sperotto, M. M., Lebrun, M. C., Tocanne, J. F., and Mouritsen, O. G. *Biophys. J.* **73**, 1940–1953 (1997).

[43] Marčelja, S. *Biophys. Biochim. Acta.* **455**, 1–7 (1976).

[44] Parsegian, V. A. and Gingell, D. *Biophys. J.* **12**, 1192–1204 (1972).

[45] Tarahovsky, Y. S., Khusainova, R. S., Gorelov, A. V., Nicolaeva, T. I., Deev, A. A., Dawson, A. K., and Ivanitsky, G. R. *FEBS Letters* **390**, 133–136 (1996).

[46] Verwey, E. J. W. and Overbeek, J. T. G. *Theory of the stability of lyophobic colloids.* Elsevier, Elsevier, New York, (1948).

[47] Andelman, D. In *Structure and Dynamics of Membranes,* Lipowsky, R. and Sackmann, E., editors, volume 1B, chapter 12, 603–642. Elsevier, Amsterdam (1995).

[48] Sackmann, E. In *Structure and Dynamics of Membranes*, Lipowsky, R. and Sackmann, E., editors, volume 1A, chapter 1, 1–64. Elsevier, Amsterdam (1995).
[49] Koltover, I., Rädler, J. O., and Safinya, C. R. *Phys. Rev. Lett.* **82**, 1991–1994 (1999).
[50] Mitrakos, P. and Macdonald, P. M. *Biochemistry* **35**, 16714–16722 (1996).
[51] Crowell, K. J. and Macdonald, P. M. *J. Chem. Phys. B* **102**, 9091–9100 (1998).
[52] Hill, T. L. *Introduction to Statistical Thermodynamics*. Addison-Wesley, New-York, (1960).
[53] Schiessel, H. *Eur. Phys. J. B* **6**, 373–380 (1998).
[54] Schiller, P. *Mol. Phys.* **98**, 493–503 (2000).
[55] Simons, K. and Ikonon, E. *Nature* **387**, 569–572 (1997).
[56] Simons, K. and Toomre, D. *Nature reviews/MCB* **1**, 31–216 (2000).
[57] May, S., Harries, D., and Ben-Shaul, A. *Phys. Rev. Lett.* **89**, 268102 (2002).
[58] Morein, S., Strandberg, E., Killian, J. A., Persson, S., Arvidson, G., Koeppe, R. E., and Lindblom, G. *Biophys. J.* **73**, 3078–3088 (1997).
[59] van der Wel, P. C. A., Pott, T., Morein, S., Greathouse, D. V., Koeppe, R. E., and Killian, J. A. *Biochemistry* **39**, 3124–3133 (2000).
[60] Killian, J. A. *Biophys. Biochim. Acta.* **1376**, 401–416 (1998).
[61] Marčelja, S. *Biophys. J* **76**, 593–594 (1999).
[62] Huang, H. W. *J. Phys. II France* **5**, 1427–1431 (1995).
[63] Lin, J.-H. and Baumgärtner, A. *Biophys. J.* **78**, 1714–1724 (2000).
[64] Bloomfield, V. A. *Curr. Opin. Struc. Biol.* **6**, 334–341 (1996).
[65] Rau, D. C. and Parsegian, V. A. *Biophys. J.* **61**, 246–259 (1992).
[66] Cerritelli, M. E., Cheng, N., Rosenberg, A. H., McPherson, C. E., Booy, F. P., and Steven, A. C. *Cell* **91**, 271–280 (1997).
[67] Hud, N. V. and Downing, K. H. *Proc. Nat'l. Acad. Sci. USA* **98**, 14925–14930 (2001).
[68] Smith, D. E., Tans, S. J., Smith, S. B., Grimes, S., Anderson, D. E., and Bustamante, C. *Nature* **413**, 748–752 (2001).

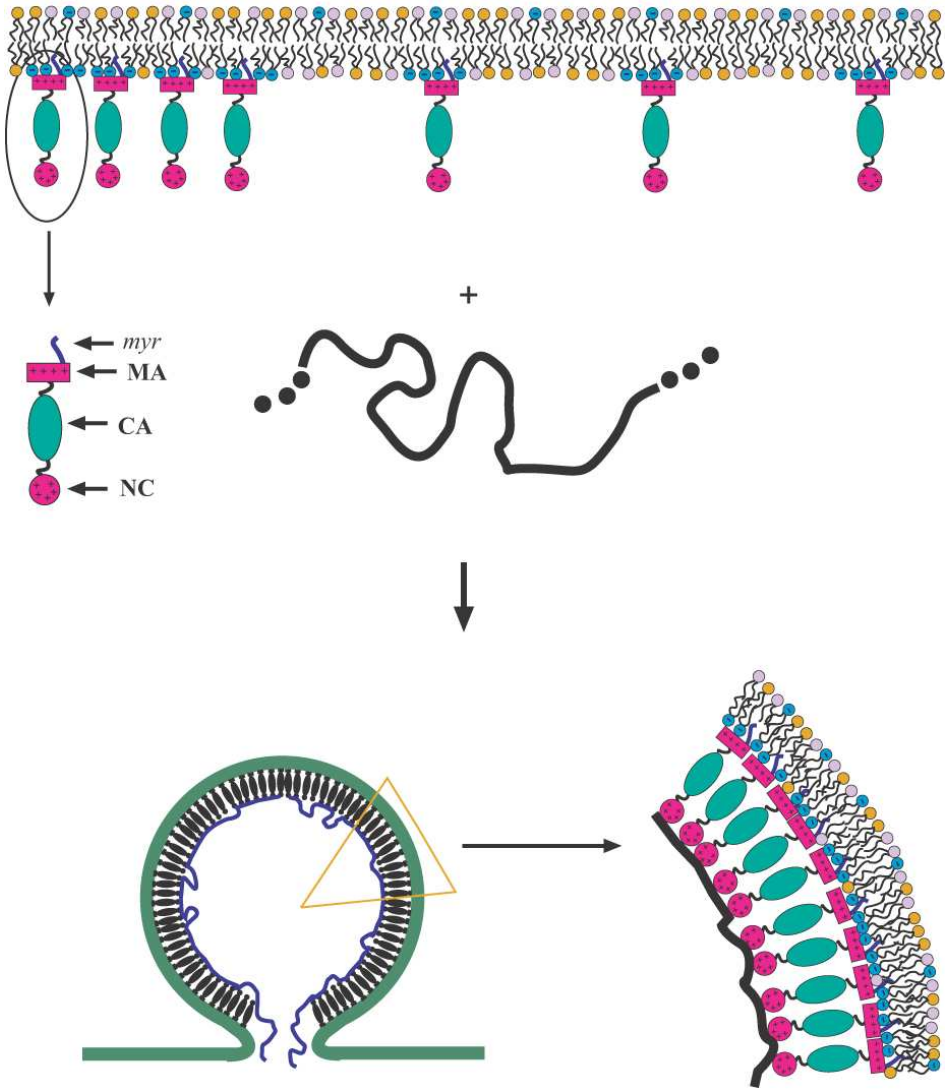

Figure 13. Schematic illustration of the budding mechanism of viruses such as C-type retroviruses, whose nucleocapsids are assembeled at the lipid-protein membrane. Top: Gag (precursor) protein complexes adsorb electrostatically, and "hydrophobically" (through a myristoyl anchor) onto the cytoplasmic surface of the plasma membrane. Lateral aggregation of the Gag complexes may occur prior to the arrival of the RNA (top left). Bottom: electrostatic binding of the ssRNA genome to the nucleocapsid domains of the Gag complexes, possibly inducing membrane curvature and budding.